

## RESEARCH ARTICLE OPEN ACCESS

Perichordal Vertebral Column Formation in *Rana kobai*Yu Takahashi<sup>1,2</sup>  | Takeshi Igawa<sup>3</sup> | Chiyo Nanba<sup>3</sup> | Hajime Ogino<sup>3</sup>  | Hideho Uchiyama<sup>2</sup> | Satoshi Kitajima<sup>1</sup>

<sup>1</sup>Division of Molecular and Cellular Toxicology, Center for Biological Safety and Research, National Institute of Health Sciences, Kawasaki, Kanagawa Prefecture, Japan | <sup>2</sup>Department of Life and Environment System Science, Graduate School of Nanobioscience, Yokohama City University, Yokohama, Kanagawa Prefecture, Japan | <sup>3</sup>Amphibian Research Center, Hiroshima University, Higashihiroshima, Hiroshima Prefecture, Japan

**Correspondence:** Yu Takahashi ([yutak@nihs.go.jp](mailto:yutak@nihs.go.jp))**Received:** 20 January 2025 | **Revised:** 13 March 2025 | **Accepted:** 21 March 2025**Keywords:** Anura | centrum | Rana | vertebral column

## ABSTRACT

The vertebral column of anurans exhibits morphological diversity that is often used in phylogenetic studies. The family *Ranidae* is one of the ecologically most successful groups of anurans, with the genus *Rana* being distributed broadly in Eurasia. However, there are relatively sparse detailed studies on the development of the vertebral column in *Rana* species, and images of the entire axial skeleton have seldom been illustrated till date. Here, we provide an illustrated description on the development of the entire vertebral column in *Rana kobai*, a Japanese small frog from the Amami Islands. Our observation of double-stained skeletal specimens revealed that in *R. kobai*, the original atlas and the first dorsal are fused into one vertebra, and the ninth neural arch is fused with the tenth arch in half of the examined larvae. Anuran vertebral column development is classified into two modes, perichordal and epichordal. *Rana* species undergo the typical perichordal mode of centrum formation. Kemp and Hoyt (1969) described that centrum formation in *R. pipiens* starts from a saddle-shaped bone on the dorsal half of the notochord. Nevertheless, our detailed observations revealed that centrum ossification initially emerges at the base of the paired neural arches and then forms the saddle-shaped bone. In *Xenopus*, a species with epichordal centra, centrum formation starts from a pair of ovoid bone elements at the base of the neural arches. Overall, our results imply that centrum ossification starts from the base of neural arches in anurans, irrespective of whether it is perichordal or epichordal. Our observations also revealed the presence of the crescent-shaped cartilage domain in the intervertebral region in *R. kobai*. The location of the crescent-shaped domain in *R. kobai* is consistent with that of the intercentrum in *Ichthyostega* and several temnospondyls. Based on our observations, we propose a hypothesis on the difference between perichordal and epichordal modes in light of evolution.

## 1 | Introduction

The vertebral column of anurans exhibits morphological diversity that is often utilized in phylogenetic studies (Nicholls 1916; Noble 1922; Griffiths 1963). This diversity has attracted interest from many authors, and quite a few studies have accumulated on the development of the vertebral column of several anuran species (Mookerjee 1931; Kemp and Hoyt 1969; Wiens 1989; Pügener and Maglia 1997; Maglia and Pügener 1998; Hall and Larsen 1998; Haas 1999; Trueb et al. 2000; Sheil and Alamillo 2005; Banbury and Maglia 2006; Pügener and

Maglia 2009; Коваленко and Кружкова 2013; Vera and Ponssa 2014; Muzzopappa et al. 2016; Soliz and Ponssa 2016). Recent studies on the development of the vertebral column in anurans include specialized species with unusual morphology or life history, such as those exhibiting extremely developed caudal vertebrae in fossorial tadpoles and direct-developing frogs (Senevirathne et al. 2016; Haas et al. 2006; Handrigan et al. 2007; Handrigan and Wassersug 2007b; Meza-joya et al. 2013), but also include large-scale analysis of common frogs for anomaly (Коваленко and Кружкова 2013; Haas et al. 2021) and locomotor types (Soliz and Ponssa 2016).

This is an open access article under the terms of the [Creative Commons Attribution-NonCommercial](https://creativecommons.org/licenses/by-nc/4.0/) License, which permits use, distribution and reproduction in any medium, provided the original work is properly cited and is not used for commercial purposes.

© 2025 The Author(s). *Journal of Morphology* published by Wiley Periodicals LLC.

The family *Ranidae* is one of the most successful groups in anurans with a distribution in most continents. In particular, the genus *Rana* includes 54 species and is the most popular frog group in temperate Eurasia (Frost 2024). Nevertheless, there are relatively sparse detailed studies on the development of the axial skeleton in *Rana* species.

Mookerjee (1931) investigated in detail the development of vertebral columns in several anuran species, including *Rana temporaria* (Mookerjee 1931). However, because his description was based on histological sections, the image of the entire axial skeleton of this species in each developmental stage was not presented in the illustrations. Thus, his study lacked details on the timing of the appearance and morphology of each neural arch and centrum as well as other skeletal elements such as the transverse process.

Kemp and Hoyt (1969) described the process of ossification in the development of the vertebral column in *Rana pipiens* using Alizarin red-stained whole mount skeletal specimens. Their observations were limited to bone ossification and not cartilage differentiation. Furthermore, although they provided a detailed description of the developmental patterns in skull ossification, they did not present illustrations on the development of the vertebral column.

Ročková and Roček (2005) prepared Alizarin red–Alcian blue double-stained skeletal specimens from several anuran species, including *Rana dalmatina*. However, they described only the development of the pelvic girdle and postsacral vertebrae and not the detailed developmental process of the entire vertebral column. Hence, their study lacked details on the developmental processes of the cervical and dorsal vertebrae and other skeletal elements. Therefore, the developmental process of the entire axial skeleton in *Rana* has seldom been illustrated to date.

According to Handrigan and Wassersug (2007a), the development of the anuran vertebral column is classified into two modes, perichordal and epichordal. In both modes, sclerotomal cells migrate and surround the notochord to form a perichordal tube. In the perichordal mode, the tube undergoes chondrification and eventual ossification around the entire circumference of the notochord. Conversely, the epichordal mode involves the cartilaginous layer and bony element formation solely on the dorsal half of the notochord, leading to notochord degeneration. In our previous paper, we described the epichordal mode of vertebral column development in *Xenopus laevis* (Takahashi et al. 2024). For comparison, we need a detailed examination of the development of the vertebral column in a perichordal species to fully understand the difference between epichordal and perichordal modes. In this study, we (1) provide a description on the development of the entire vertebral column in *R. kobai*, a small Japanese frog from the Amami-Oshima Island, and (2) discuss possible implications on centrum formation in perichordal and epichordal modes in an evolutionary background.

## 2 | Materials and Methods

### 2.1 | Animals

Adult individuals of *Rana kobai* were obtained from Ogachi, Amami-Oshima Island, in March 2017, that have been reared at

the Amphibian Research Center, Hiroshima University. Female and male individuals were housed in the same cage, and offspring were obtained by natural breeding. The pair of F1 individuals laid 230 fertilized eggs in 2020, and we reared them by feeding them on boiled spinach after they hatched.

Larvae were staged according to Tahara (1974). The number of samples at each stage (St.) is as follows: St. 27, 5; St. 29, 5; St. 31, 5; St. 33, 5; St. 35, 5; St. 37, 6; St. 38, 6; and St. 40, 5. All animal experiments were conducted according to the Guidelines for Proper Conduct of Animal Experiments (2006. 6. 1 Science Council of Japan).

### 2.2 | Skeletal Preparations

Alcian blue–Alizarin red cartilage–bone double staining was performed using a modification of an established method (Yasutake et al. 2004). Briefly, *Rana* larvae were fixed overnight in 10% formalin at 4°C. After rinsing with distilled water, the samples were stored in 70% ethanol at 4°C. Careful skinning and evisceration of the samples followed, and they were further preserved in 70% ethanol. Cartilage was stained overnight with Alcian blue solution at room temperature. Then, the samples were subjected to a graded ethanol series followed by trypsin treatment for 3 days with daily trypsin solution changes. The digested samples were washed in 0.5% potassium hydroxide (KOH) and then stained overnight with Alizarin red solution at room temperature. After washing in 0.5% KOH, the samples were bleached with hydrogen peroxide for 4 h and processed in a graded series of 0.5% KOH/glycerol. The cleared specimens were observed and photographed in 80% glycerol before final storage in 100% glycerol. If necessary, skeletal dissection was performed using sharp tweezers, after which observations were made and photographs were captured using a Leica binocular stereomicroscope and an Olympus DP-74 digital camera, respectively.

### 2.3 | Identification and Designation of Skeletal Elements

The vertebral column of most extant anurans consists of 12 vertebral primordia. In contrast to the adult vertebral column of *Rana temporaria* (Mookerjee 1931), the atlas and the first dorsal are fused into one; hence, we referred to this vertebra as 1 + 2 (see Section 4). We confirmed all vertebral elements in St. 40 metamorphosed froglets and compared them with the elements in earlier stages successively.

To facilitate clarity, we prefer using Arabic numerals (1, 2, 3, etc.) instead of traditional Roman numerals for labeling the vertebral elements in figures, as the latter can vary in character length (e.g., I and VIII or XII), making them unsuitable for labeling. In the text, we refer to the vertebral elements as the 1st to 12th vertebrae.

## 3 | Results

### 3.1 | Neural Arch Development

Cartilaginous neural arch primordia develop earliest among all vertebral skeletal elements. In this section, we present an

overview of the development of the neural arch, and subsequent ossification of the arches and centrum formation are described in the next section. Development of the postsacral vertebrae and urostyle are described in a separate section.

In St. 27, almost no vertebral elements were detected; however, in some larvae, faint cartilage staining of the lamina primordia was visible at the dorsal side of neural arches (Figure 1a). These primordia were arranged as three pairs probably representing the third, fourth, and fifth laminae of neural arches, respectively, based on their relative positions. This is consistent with the early stage of neural arch development in *Xenopus laevis* (Takahashi et al. 2024). We did not examine St. 28 larvae because of the limitation of samples.

In St. 29, seven pairs of neural arch primordia were observed (Figure 1b,c). As the first pair appeared initially single, but later bifurcated, we designate it here as 1 + 2. In the early St. 29 larvae, the third, fourth, and fifth pairs of neural arch primordia were larger than those of the others, and the eighth pair showed only rudimentary staining. All neural arches were oriented dorsally (Figure 1b). In the late St. 29 larvae, the neural arch primordia grew dorsally, and the fourth and fifth pairs oriented posterodorsally at their distal ends (Figure 1c).

In St. 31, the eighth pairs of neural arch primordia were clearly observed and numbered from 1 + 2 to 9 (Figure 1d). The ventral portion (pedicle) remained vertical, whereas the dorsal portion (lamina) was oriented posterodorsally in most arches. Here,

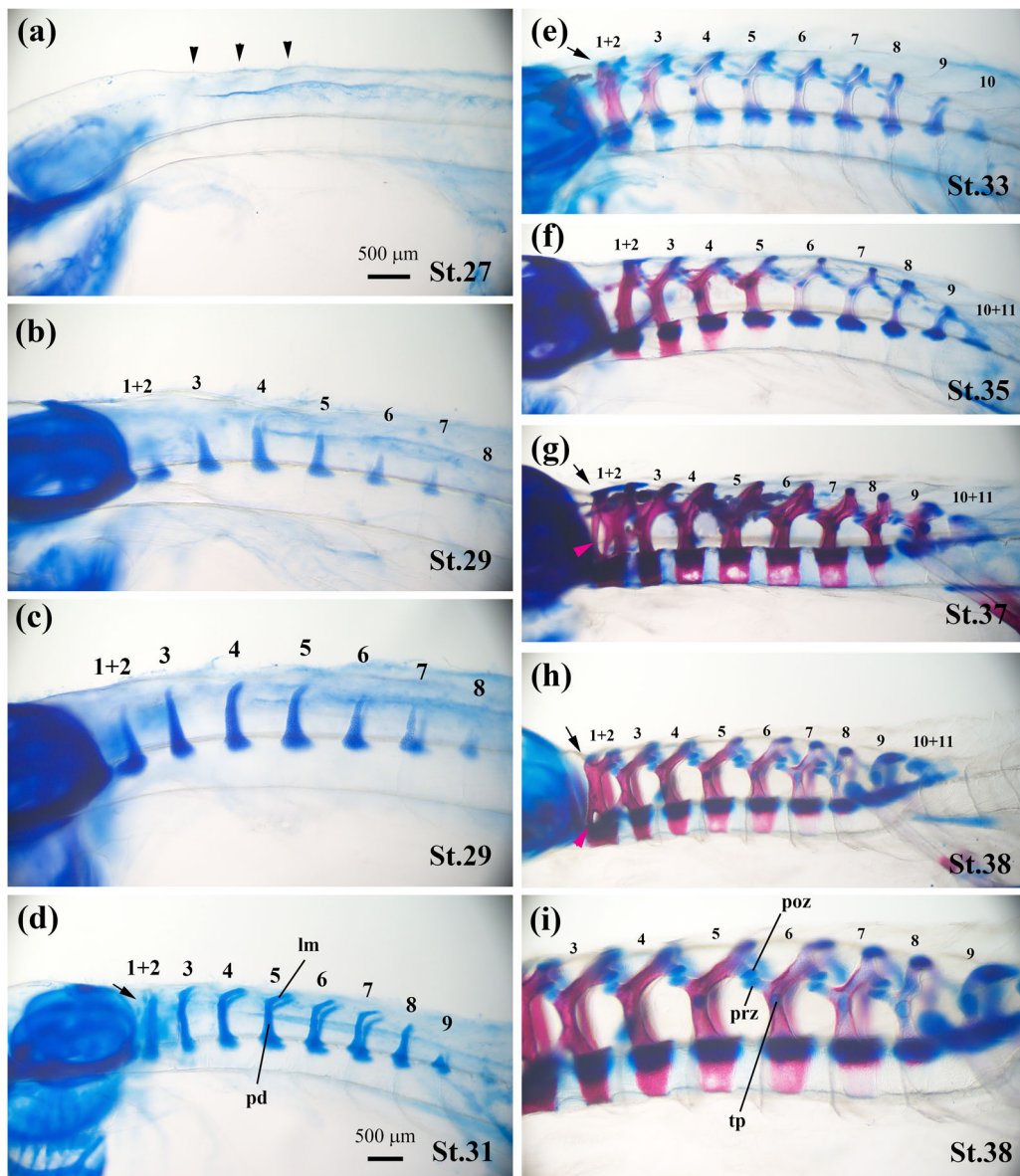


**FIGURE 1** | Overview of neural arch development in *Rana kobai*. Lateral views of (a) St. 27, (b) early St. 29, (c) late St. 29, (d) St. 31, (e) St. 33, (f) St. 35, (g) St. 37, (h) St. 38, and (i) higher magnification of St. 38 larvae. Arrowheads in (a) indicate three pairs of lamina primordia. Arrows in (d), (e), (g), and (h) show the bifurcation of the distal ends of the 1 + 2 arches. Magenta arrowheads show the remains of spinal foramina. lm, lamina; pd, pedicle; poz, postzygapophysis; prz, prezygapophysis; tp, transverse process. The scale bar in (a) is common among (a), (b), (c), and (i). The scale bar in (d) is common among (d) to (h).



dorsal bifurcation of 1 + 2 arches was observed. The primordia of the prezygapophysis began developing at the anterior margin of the third to sixth arches (Figures 1d and 2).

In St. 33, the primordia of the postsacral neural arch (the tenth) were added posteriorly, and the articular processes (prezygapophysis and postzygapophysis) clearly developed to connect the consecutive arches (Figure 1e). Transverse processes also began developing at most of the arches. In St. 35–37, slightly wide postsacral neural arches (10 + 11) emerged posteriorly, and this state continued as late as St. 38 (Figure 1f–h). The twelfth arch emerged later at St. 38–40 (Figure 5). As the ossification of neural arches proceeded, most of the pedicle and lamina were ossified; however, the articular and transverse processes remained cartilaginous (Figure 1e–i).

### 3.2 | Ossification of Neural Arches and Formation of the Centrum

The ossification of neural arches proceeded posteriorly, which was followed by centrum formation. In St. 31, all neural arches were cartilaginous, and no sign of centrum primordia was observed around the notochord (Figures 2a and 3a). In St. 33, a series of developmental stages was observed on centrum formation at the anterior vertebrae. In early St. 33 larvae, the pedicle of the arches began calcifying but stained only faintly pink (Figure 2b). In the lateral and ventral views, cartilaginous cylindrical centrum primordia were observed around the notochord (Figures 2b and 3b), and these centrum primordia were detected up to the sixth or seventh vertebra. When the anteriormost two pairs of neural arches were ossified and stained strongly, the initial sign of centrum ossification was detected at the base of the first (1 + 2) arches (Figures 2c and 3c). When the anterior three pairs of the arches were strongly stained, centrum ossification was observed at the base of the anterior two or three pairs of the arches (Figures 2d and 3d). When the anterior four pairs of the arches were strongly stained, centrum ossification was detected at the base of the anterior three pairs of the arches (Figures 2e and 3e). At this stage, ossification expanded medially from the base of neural arches to the dorsal side of the notochord at the anterior two vertebrae (1 + 2 and 3). The paired ossification domains at the fourth vertebra were still separated from each other. In St. 35, centrum ossification proceeded posteriorly, and its extent varied among individuals. In early St. 35 larvae that showed strong ossification at the anterior four pairs of the arches, centrum ossification was cylindrical at the anterior three (1 + 2, 3, 4), that is, ossification reached the ventral side of the notochord. Here, the ossification domain at the fifth centrum remained at the dorsal side of the notochord (Figures 2f and 3f). Similarly, when the anterior five pairs of the arches were strongly stained, centrum ossification was cylindrical at the anterior four (1 + 2, 3, 4, 5; Figures 2g and 3g). When the anterior six pairs of the arches were strongly stained, centrum ossification was cylindrical at the anterior five (1 + 2, 3, 4, 5, 6; Figures 2h and 3h). At St. 37, ossification of the arches reached the ninth vertebra (sacrum), and centrum ossification was cylindrical up to the seventh vertebra (Figures 2i and 3i). Centrum ossification at the eighth was not cylindrical; however, its anterior–posterior length was short at the ventral side, showing

an inverted triangle in the lateral view (Figure 2i). Finally, at St. 40, the eighth centrum was still not cylindrical, and often the ossification did not reach the ventral end of the notochord. The ninth centrum exhibited ossification; however, its ossified domain was localized at the base of the arches and dorsal side of the notochord, with only a small area expanding laterally (Figures 2j and 3j). Even at St. 40, the ninth centrum was not cylindrical, and bilateral ossifications were separated (Figure 3j).

Regarding centrum formation at the posterior trunk, a step-by-step formation of the cylindrical centrum is shown in Figures 2 and 3. However, not all individuals may undergo this trajectory. Some larvae exhibited delayed formation of the sixth and seventh centra, so that ossification did not cover the ventral side of the notochord at the sixth to eighth centra even at St. 40 (Figure 4).

### 3.3 | Development of the Intervertebral Region

In anuran species with perichordal formation of the vertebral column, the cylindrical vertebral region and intervertebral region alternate around the notochord (Handrigan et al. 2007). The vertebral region ossifies to form the centrum, whereas the intervertebral region remains cartilaginous. As in other species, the intervertebral region develops later than the centrum in *R. kobai*.

In St. 33, when the cartilaginous centrum primordia emerged around the notochord, no cartilage was detected between the neighboring centra (Figure 2b–e). This situation continued to St. 35 when centrum ossification proceeded posteriorly (Figure 2f–h). At St. 37, a relatively uniform cartilage staining was observed between the ossified centra (Figure 2i). From St. 38 to 40, a regional difference was detected in the intervertebral region. In a St. 40 metamorphosed froglet, strongly stained cartilage domains were observed posteroventral to each centrum (Figure 4a), which were conspicuous at regions posteroventral to the fifth, sixth, and seventh centra (arrowheads). Cartilage domains anteroventral to the centra were also detected, but these were less conspicuous. The domain posteroventral to each centrum appeared wedge-shaped in the lateral view, indicating a crescent shape surrounding the ventral side of the notochord. In fact, in the ventrolateral view, this domain consisted of a pair of crescents occasionally connected at midline (Figure 4b, white arrowheads). In another St. 40 froglet, the cartilage domain was conspicuous at regions posteroventral to the fourth, fifth, and sixth centra (Figure 4c, arrowheads). This regional difference was constantly observed in one St. 38 larva and most St. 40 froglets. This crescent-shaped domain probably represents the primordium of the intervertebral disc in *Rana* but does not resemble the previously reported cartilaginous socket or ball in *R. temporaria* (Mookerjee 1931).

### 3.4 | Development of Postsacral Vertebrae and Urostyle

Postsacral vertebrae (10, 11, 12), which possess only neural arches and lack centra, combine with the hypochord under the notochord to form the urostyle. Postsacral neural arches

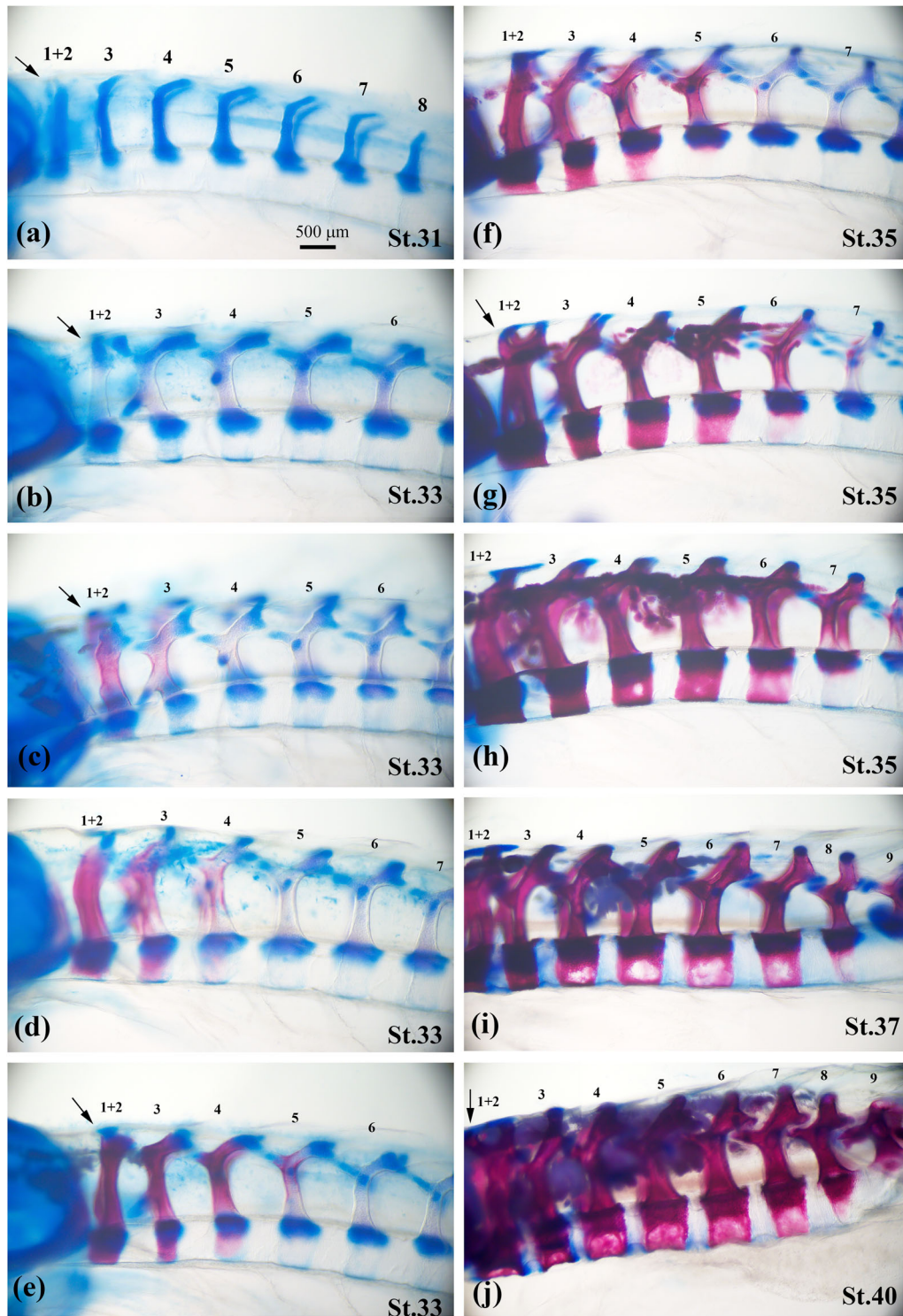


**FIGURE 2** | Progression of neural arch ossification and centrum formation in the lateral view of *Rana kobai* larvae. (a) St. 31, (b–e) St. 33, (f–h) St. 35, (i) St. 37, and (j) St. 40 larvae. Arrows in (a), (b), (c), (e), (g), and (j) show the bifurcation or abnormal shape of the lamina of the 1 + 2 arches. The scale bar in (a) is common among (a) to (j).

emerged as mutually fused cartilage, and independent 11th or 12th arches were never observed. In St. 35, the 10th portion of the cartilage emerged posterior to the ninth arch (Figure 5a,b,e). In a larva in Figure 5a, there is only the 10th portion on the left side and a long cartilage (10 + 11) on the right side. At St. 37, the 11th portion emerged and was added to the posterior of the 10th portion (Figure 5c,f). Between the

10th and 11th portions, a small foramen (spinal foramen) was observed. In St. 38, the 12th portion emerged, and some larvae showed the 10th, 11th, and 12th portions, each demarcated with small spinal foramina between them (Figure 5g). In St. 40, the 10 + 11 portion was a completely fused structure, and a spinal foramen was observed between the 10 + 11 and the 12th portion (Figure 5d,h).



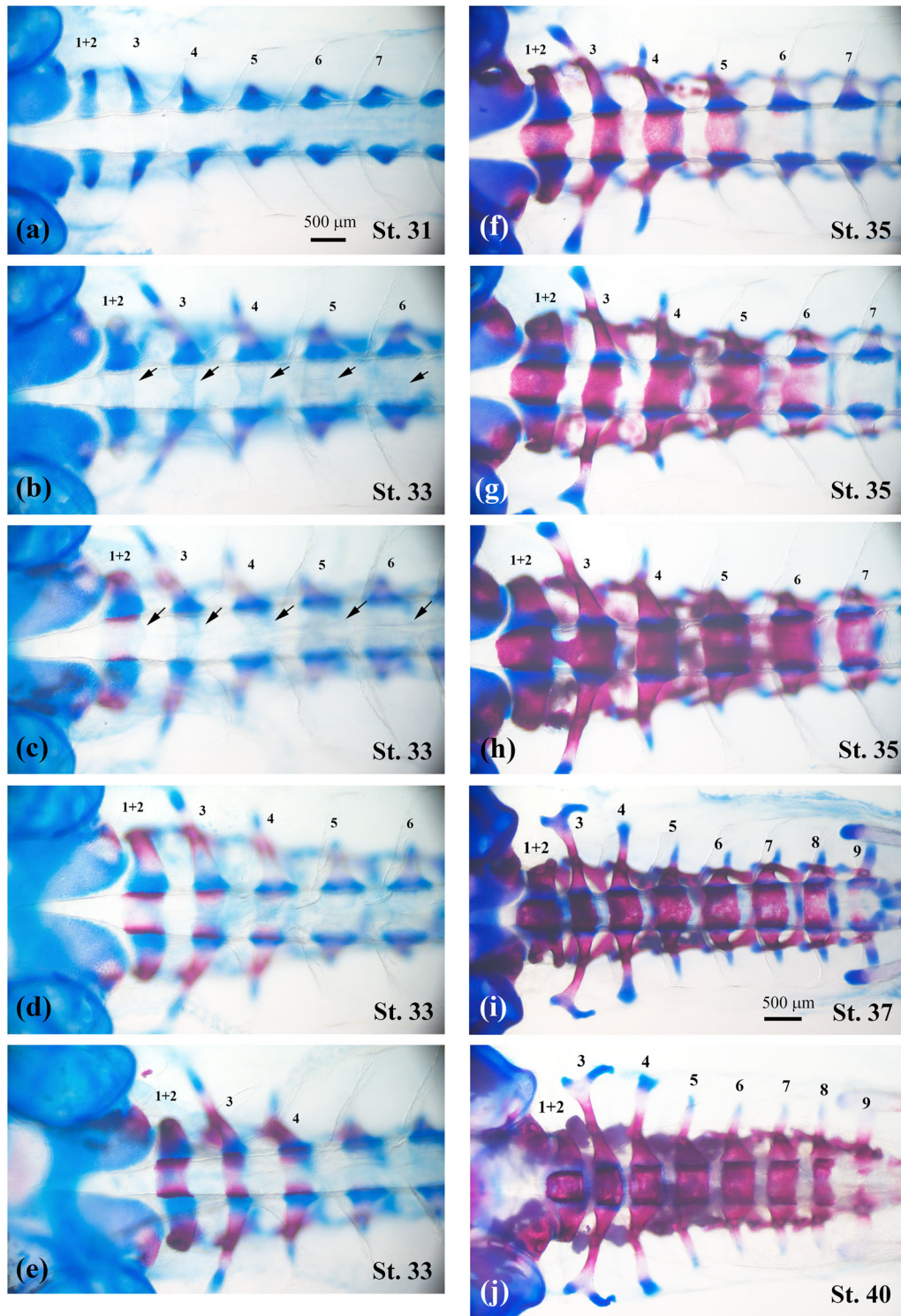


**FIGURE 3** | Progression of neural arch ossification and centrum formation in the ventral view of *Rana kobai* larvae. (a) St. 31, (b–e) St. 33, (f–h) St. 35, (i) St. 37, (j) and St. 40 larvae. Arrows in (b) and (c) indicate the cartilaginous cylindrical centrum primordia. The scale bar in (a) is common among (a) to (h). The scale bar in (i) is common between (i) and (j).

The *R. kobai* population examined in our study demonstrated variation (polymorphism) in the relationship between the ninth and 10th arches. One type demonstrated fusion between the ninth and 10th arches (Figure 5a–d), wherein the lamina of the ninth arch inclined posteriorly and fused with the 10th portion of the postsacral vertebrae. Moreover, the ninth arch tended to lack the prezygapophysis for articulation with the eighth arch

(Figure 5b–d). In the other type, the ninth arch was independent and separated from the postsacral vertebrae (Figure 5e–h). In this case, the lamina of the ninth arch was relatively vertical, and the prezygapophysis of the ninth arch was retained to articulate with the eighth arch (Figure 5f–h). The final morphology of the two types was the integration of the ninth arch into the urostyle in the first type (Figure 5d) and separation

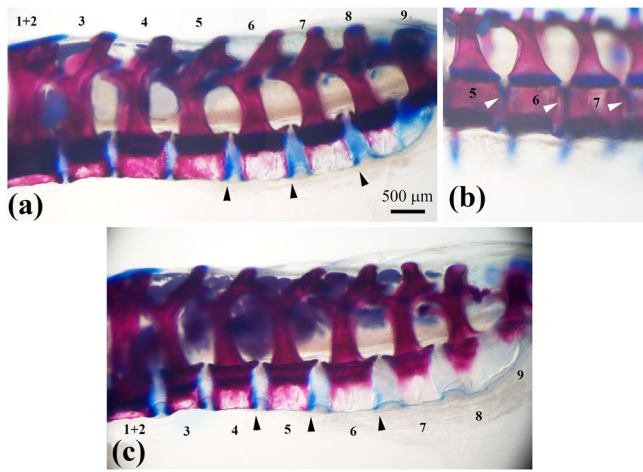


**FIGURE 4** | Regionalization of the intervertebral region during the larval development of *Rana kobai*. (a) A St. 40 froglet showing a wedge-like cartilage domain posteroventral to each centrum (arrowheads). (b) the same froglet as in (a), showing crescent-shaped domains (white arrowheads) ventral to the notochord in the ventrolateral view. (c) Another St. 40 froglet showing a wedge-like cartilage domain posteroventral to each centrum (arrowheads). The scale bar in (a) is common among (a) to (c).

with a large gap between the ninth arch and urostyle in the second type (Figure 5h). The ratio of the number of the first and second types was 1:1 among the examined samples.

In St. 35, the hypochord emerged at the ventral side of the notochord and largely spanned the anteroposterior range of the postsacral vertebrae (Figure 5a,b,e). In St. 37, the hypochord elongated posteriorly (Figure 5c,f). At St. 38–40, the posterior end of the hypochord lied further posteriorly to the 12th portion of the postsacral vertebrae (Figure 5d,g,h). Until St. 38, the notochord was extremely thick at the tail region (Figure 5a,b,c,e,f,g). From St. 38 to 40, the notochord regressed, and the postsacral cartilage and hypochord approached but did not fuse with each other (Figure 5d,h). Until St. 35, the hypochord was entirely cartilaginous. At St. 37–38, the ventral side of the hypochord began calcifying (Figure 5c,f,g). At St. 40, most of the hypochord ossified, leaving the posterior end being cartilaginous (Figure 5d,h).

### 3.5 | Development of Ribs and Transverse Processes

In some ancestral anurans, the thoracic rib is considered as the original rib fused with the transverse process (diapophysis). In *Rana*, all dorsal and sacral vertebrae possess a transverse process (Mookerjee 1931).

Until St. 29, there was no sign of the transverse process at the lateral portion of neural arches. At St. 31, small, pointed, and anterolaterally directed processes were observed at the lateral side of the third and fourth neural arches (Figure 6a). The remaining neural arches lacked such remarkable protrusions and exhibited only round surfaces. In St. 33, the articular processes clearly developed, and transverse processes began emerging as small lateral protrusions at most of the neural arches (Figure 6b). The 1 + 2 vertebra often lacked transverse

processes. The third and fourth transverse processes were obviously larger than the fifth to eighth; the third transverse process oriented anterolaterally, and the fourth oriented laterally. The fifth to eighth transverse processes were small and triangular. In St. 35, the third and fourth transverse processes further developed as a rib-like structure, whereas the fifth to eighth remained small and triangular (Figure 6c). The ninth process emerged as a small triangular protrusion. The third process often bifurcated at the distal end with anterior and posterior directed prongs. Thus, until St. 35, *Rana* larva appeared to have only two or three pairs of ribs. In St. 37, the third and fourth processes grew further, and the fifth to eighth processes began to elongate laterally (Figure 6d). The ninth process developed to articulate with the ilia and were now larger and more robust than the fifth to eighth processes. In St. 40, the third and fourth processes were the largest, and the fifth to eighth processes also developed as long, rib-like structures (Figure 6e). The 1 + 2 transverse process (when present) was straight and oriented anterolaterally, the third process was strongly hooked posteriorly with an anteriorly directed accessory prong, and the fourth process was slightly expanded distally. The fifth to eighth processes were almost straight and oriented posterolaterally or laterally. The ninth process was the most robust.

## 4 | Discussion

In the current study, vertebral column development and especially the process of centrum formation in *R. kobai* was illustrated in whole-mount skeletal specimens. Formation of the centrum and intervertebral cartilage around the notochord in *Rana* was visualized in color photographs for the first time. The typical perichordal mode of centrum formation in *Rana* highlights the peculiarity of epichordal centrum formation in *Xenopus* demonstrated in our previous study (Figure 7; Takahashi et al. 2024).

### 4.1 | Reduction of Vertebral Number in *R. kobai*

We noticed a tendency of reduction of the number of vertebrae in the axial skeleton of *R. kobai*. According to Mookerjee (1931), the adult vertebral column of *R. temporaria* is composed of one cervical (atlas), seven dorsal, one sacral, and postsacral vertebrae. The second to eighth vertebrae have long rib-like transverse processes (diapophysis), and the ninth (sacral) has long and robust transverse processes to articulate with the ilium. Among extant anurans, species in the Leiopelmatidae and Ascaphidae have nine presacral vertebrae, and all other families have eight or less (Haas 2003).

The metamorphosed froglet of *R. kobai* has only seven presacral vertebrae. Most of the examined larvae had two pairs of neural arches in the first vertebra (Figures 1, 2, and 6). Some larvae exhibit rib-like transverse processes from this vertebra, whereas others lack it, implying that this first vertebra articulates with the occiput (like cervical) and at the same time has a rib-like transverse process (like dorsal) in some larvae. Furthermore, some larvae had the remains of a spinal foramen at the base of neural arches (Figure 1). Therefore, we interpret that this



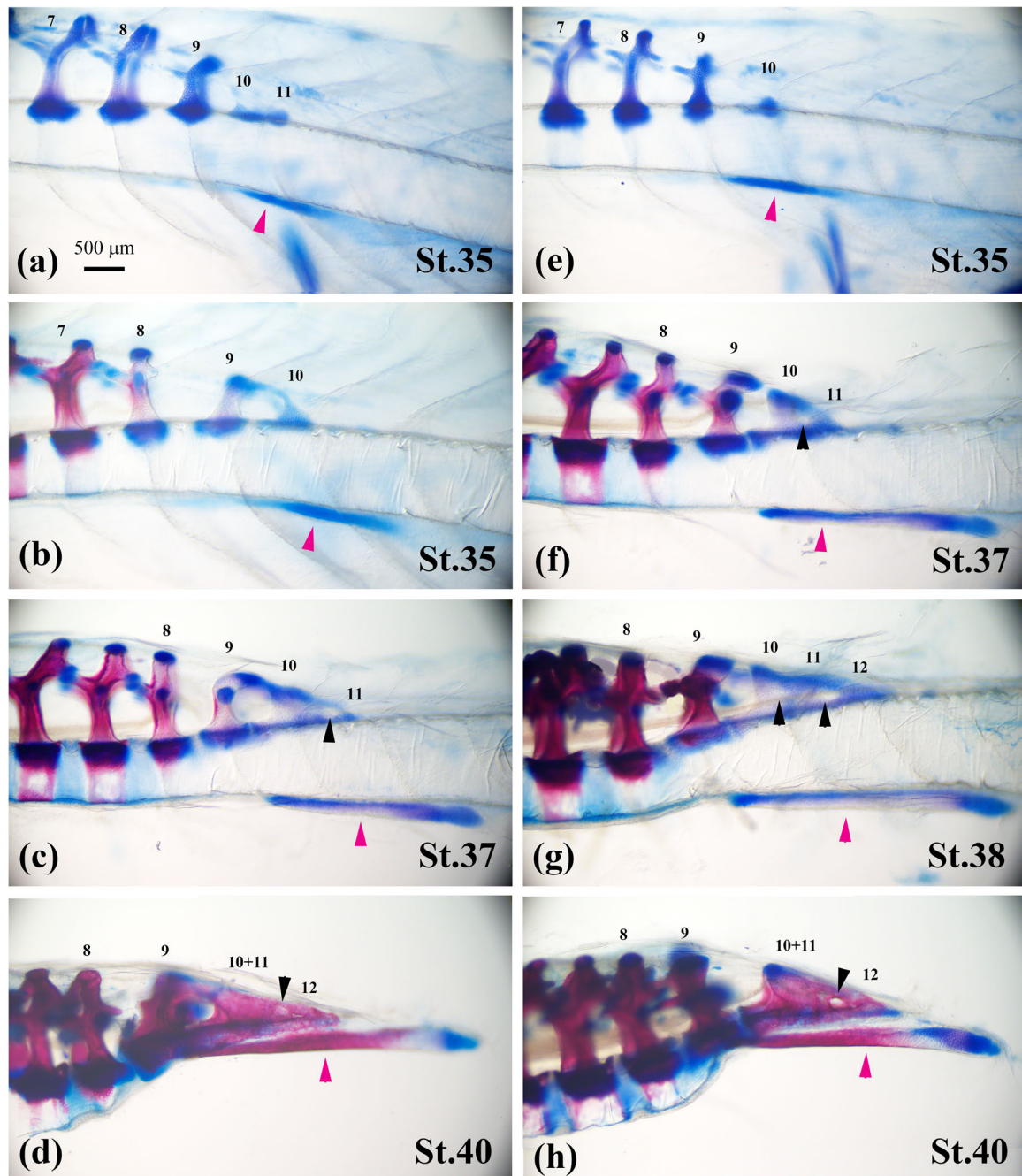


**FIGURE 5** | Postsacral vertebrae and urostyle development in *Rana kobai*. (a, b, e) St. 35 larvae with the tenth arches of postsacral vertebrae. (c, f) St. 37 larvae with 10 + 11 arches. (g) a St. 38 larva showing 10 + 11 + 12 fused arches. (d, h) St. 40 froglets exhibiting 10 + 11 + 12 fused arches and regression of the notochord resulting in closure of postsacral arches and the hypochord. Here, two morphotypes are presented; (a–d) Fusion type, in which the ninth arch fuses with the tenth arch. (e–h) Separate type, in which the ninth arch is separated from the tenth arch. The difference in the relationship between the ninth and tenth arches in each type is shown (d, h). Black arrowheads, spinal foramina; magenta arrowheads, hypochord. The scale bar in (a) is common among (a) to (h).

vertebra is a complex formed by the fusion of the original atlas and the first dorsal (1 + 2), which may be an unusual feature of *R. kobai* among *Rana* species. The morphology of the two pairs of neural arches at this 1 + 2 vertebra is variable, that is, the first arch is separated from the second arch, or they exhibit a bifurcated form. During the development of the neural arch, the second arch appears first and then the first arch is added. Mookerjee (1931) described that in the initial development of the neural arch in *R. temporaria*, an intercalated arch appears

between the occipital arch and the atlas arch proper, which later fuses with the latter, probably indicating that the atlas was originally formed by the fusion of two elements. However, the species in this study has a normal, independent atlas, implying that the situation is different between *R. temporaria* and *R. kobai*.

Fusion of the 1st and 2nd vertebrae has been reported both in evolutionary context and in the case of developmental anomaly



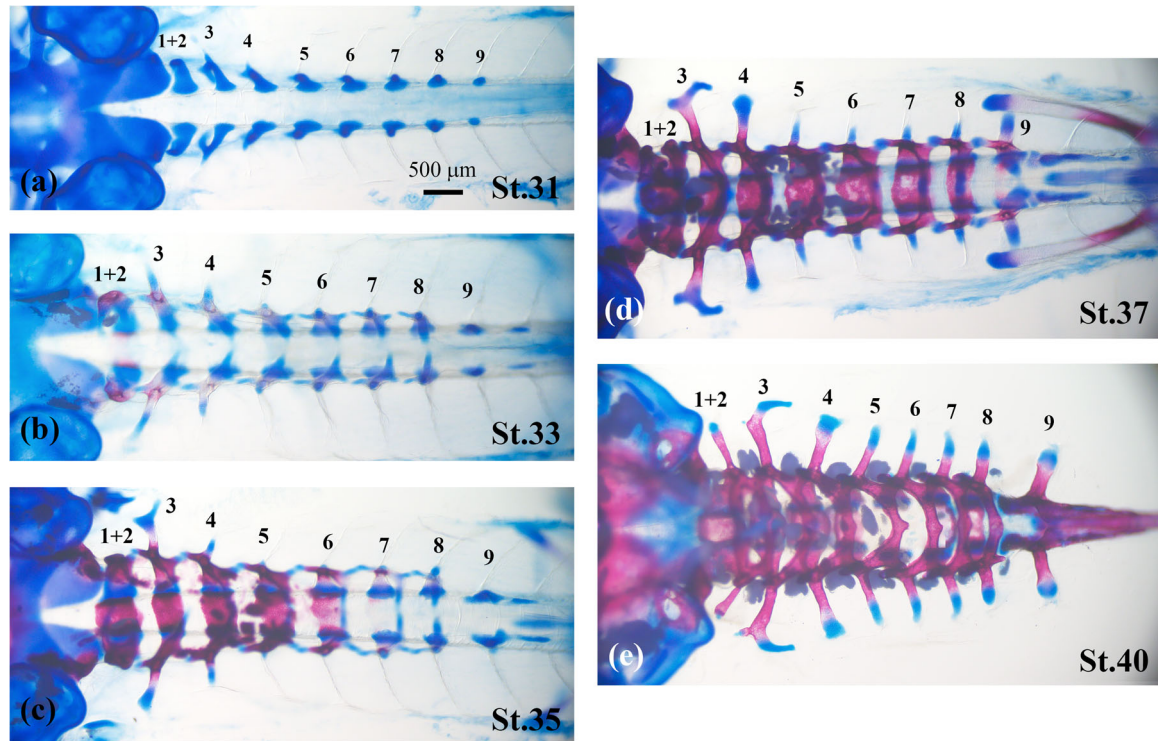


**FIGURE 6** | Rib and transverse process development in *Rana kobai*. (a) St. 31, (b) St. 33, (c) St. 35, (d) St. 37 larvae, and (e) St. 40 froglet in the dorsal view. The fifth to eighth transverse processes elongate as rib-like processes only at the late stage. The scale bar in (a) is common among (a) to (e).

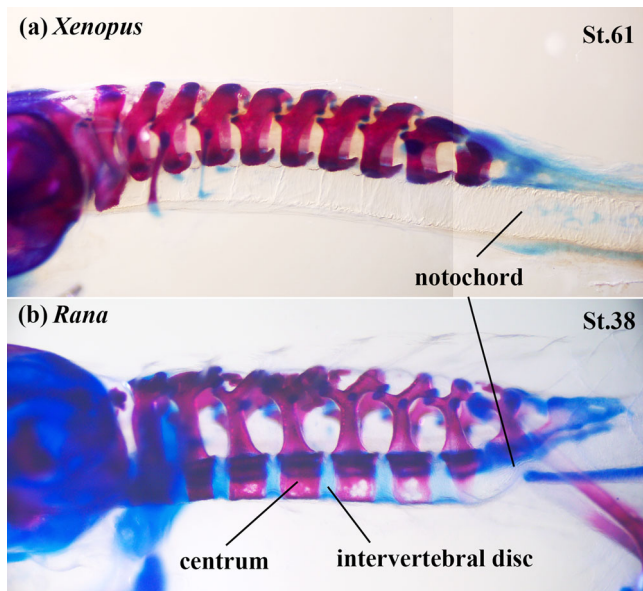


**FIGURE 7** | Difference between perichordal and epichordal modes of centrum formation shown by whole-mount skeletal specimens slightly before the completion of metamorphosis. (a) Lateral view of a *Xenopus laevis* larva at St. 61, (b) lateral view of a *Rana kobai* larva at St. 38. Note that the centrum and intervertebral region are formed around the notochord in (b) and are located dorsally to the thick notochord in (a).

(Haas et al. 2021). Anomalous fusions of the vertebrae 1 + 2 have been reported in some individuals of *Bufotes viridis* (Adolphi 1892) and *Pelobates fuscus* (Adolphi 1895). However, complete fusions of the vertebrae 1 + 2 are considered normal

in *Pipa* (Trueb et al. 2000) and *Microhyla nepenthicola* (Haas et al. 2021).

Another finding that may reflect the tendency of reduction in the number of vertebrae is that the ninth neural arch often fuses with the tenth arch of the postsacral vertebrae. Half of the examined larvae exhibited this phenomenon during urostyle development (Figure 5). Fusion of the sacral neural arch with the urostyle may have a functional significance to make the complex more rigid; however, whether this tendency is widely observed in this species is yet to be confirmed. Fusion of the ninth and tenth arches occurs in Pelobatidae species (Banbury and Maglia 2006), although the reason may differ from this case. It is interesting that *R. kobai* exhibits the vertebral fusions at the 1 + 2 and 9 + 10 positions, where vertebral anomaly occurs most frequently in various anuran species (Haas et al. 2021).

#### 4.2 | Development of Ribs and Transverse Processes

Anurans seem to have an evolutionary trend toward rib loss in the presacral region. Adult basal anurans, including extinct Jurassic species, Ascaphidae, Leiopelmatidae, and Discoglossidae possess some free ribs in the anterior presacral region (2–4th vertebrae). Some families, such as Pipidae, lack free ribs in adults as a result of fusion to the transverse processes during ontogeny. In most advanced anurans, the ribs are considered to be lost in adults (Blanco and Sanchiz 2000). Thus, *Xenopus* has ribs in the thoracic region (Trueb and Hanken 1992), whereas *Rana* has long transverse processes as

mentioned earlier. The presence of small rib rudiments at the tip of the anterior transverse processes has been reported in *Rana catesbeiana* and *R. perezi* (Blanco and Sanchiz 2000), but those rudiments were not detected in our examined samples of *R. kobai*.

In *R. kobai*, the 1 + 2, 3rd, and 4th vertebrae have long transverse processes, and the 5th to 8th vertebrae also have comparably long transverse processes in the metamorphosed froglet (Figure 6). However, having long transverse processes in the 5th to 8th vertebrae is a late-developing feature in this species. As shown in Figure 6, at an early stage of vertebral column development, the transverse processes of the 5th–8th vertebrae are extremely small, whereas those of the 1 + 2, 3rd, and 4th vertebrae are long and rib-like. Only at the late stages of development do they grow rapidly to acquire the rib-like length.

In a stem batrachian *Notobatrachus*, both adult and larval specimens are known (Báez and Nicoli 2004; Chuliver et al. 2024). The adult vertebral column has free ribs attached to the distal end of the transverse process proper in the thoracic region. Its posterior transverse processes are relatively long and much longer than the transverse processes proper in the thoracic region (Báez and Nicoli 2004). In contrast, in the tadpole, the posterior transverse processes are similar in length to the transverse processes proper in the thoracic region (Chuliver et al. 2024). Therefore, the posterior transverse processes elongate rapidly during metamorphosis and postmetamorphic development. This implies that late elongation of the posterior transverse processes in *Rana* may be a conserved pattern retained from a basal lineage of anurans.

### 4.3 | Process of Centrum Formation in Perichordal Species

Mookerjee (1931) described vertebral column formation in *Rana temporaria* from the embryonic to adult stage. However, because his observations were based on histological sections, the contents of the description do not necessarily correspond to the gross anatomical description in the present study. For instance, Mookerjee (1931) did not describe the timing of the appearance and morphology of each neural arch and centrum. Moreover, his staging of larvae was based only on their total length, making it difficult to compare with other anuran species. Therefore, a precise comparison between *R. temporaria* and *R. kobai* is difficult.

Nonetheless, his description indicates that *Rana temporaria* follows the perichordal mode, and centrum formation begins at the dorsal side of the notochord and then proceeds to the ventral side. At the “Stage 22 mm” when the first nine neural arches enveloped the spinal cord, Mookerjee (1931) stated that “In the vertebral region, the thin perichordal tube just at the base of each cartilaginous arch changes from a fibrous connective tissue layer to one row of cartilaginous cells. ... The mid-dorsal part as well as the ventral part of the perichordal tube is still fibrous.” Hence, he described that cartilage differentiation precedes at the base of neural arches in the perichordal tube; however, he did not mention from which region the centrum ossification starts in the already cartilaginous perichordal tube.

Kemp and Hoyt (1969) described that on centrum formation in *R. pipiens*, a saddle-shaped bone appears first on the dorsal half of the notochord, and then the ossification expands ventrally to surround the entire circumference of the notochord. However, our detailed observations revealed that centrum ossification initially emerges at the base of the paired neural arches and then forms the saddle-shaped bone (Figure 3). Although we cannot exclude the possibility of a species difference between *R. pipiens* and *R. kobai*, our findings suggest that a pair of ossification centers at the base of neural arches are common among *Rana* species. This process has also been reported in *Spea*, another perichordal genus (Wiens 1989; Banbury and Maglia 2006). It is worth noting that in *Xenopus*, a species with epichordal centrum formation, centrum formation initiates from a pair of ovoid bone elements at the base of neural arches (Takahashi et al. 2024). Paired ossification centers at the base of the neural arches are also reported in *Acris* (Pugener and Maglia 2009), *Scaphiopus* (Hall and Larsen 1998), *Pyxicephalus* (Haas 1999), and *Calyptocephalella* (Muzzopappa et al. 2016), in addition to the above-mentioned taxa. Taken together, these data imply that centrum ossification begins from the base of neural arches in anurans, irrespective of whether it is perichordal or epichordal.

In *R. kobai*, a pair of straight, rod-like ossification centers emerge at the base of neural arches, expand dorsally to form the saddle-shaped plate, and then expand ventrally to form a cylindrical centrum (Figure 3). In *Spea multiplicata*, a pair of small, pebble-like ossification centers appear, expand and fuse dorsally, and then expand ventrally to form a cylindrical centrum (Banbury and Maglia 2006). In *X. laevis*, a pair of ovoid ossification centers expand and fuse at the dorsal midline to form the epichordal centrum (Takahashi et al. 2024). Interestingly, the initial shape of the ossification centers is similar in *Spea* and *Xenopus*, indicating that *Spea* represents an intermediate form between *Rana* and *Xenopus*.

Another finding in the present study was the crescent-shaped cartilage domain in the intervertebral region in *Rana* (Figure 4). Kemp and Hoyt (1969) observed only bone ossification through Alizarin red staining and did not observe cartilage in *R. pipiens*. Mookerjee (1931) described that most of the trunk vertebrae of *Rana temporaria* were procoelic, and connective tissue invaded into the intervertebral cartilage at the young adult stage. However, he made no description of the ventral crescent-shaped domain at the metamorphosing larval stage. Griffiths (1963) referred to Mookerjee (1931) and clearly illustrated the development of the intervertebral disc in anurans but mentioned nothing about the crescent-shaped domain. This crescent-shaped domain localizes ventrally to the notochord in the metamorphosing tadpole and forms much earlier than the cartilaginous socket or ball formed after the inward invasion of the cartilage and constriction of the notochord (Griffiths 1963). Therefore, we interpret here that the intervertebral disc primordium emerges as the crescent-shaped domain at the initial stage and later becomes modified into the form of the cartilaginous socket and ball. Due to the limitation of samples, we could not follow up the possible dynamic morphological change in the intervertebral disc region.

However, the formation of some cartilage tissue localized ventrally to the notochord is not restricted to *Rana*. The crescent-

shaped cartilage is not detected in *Xenopus*, because the notochord itself is degenerative at later stages; however, when it is thick and robust, it has a continuous ventral cartilage layer, which is a transient structure (Mookerjee 1931; Nieuwkoop 1956; Takahashi et al. 2024). None of the previous authors discussed why this cartilage is formed at the ventral midline. The presence or absence of this ventral cartilage layer has not been investigated or reported in other species with epichordal centrum formation (*Bombina* (Maglia and Pugener 1998); *Pipa* (Trueb et al. 2000); *Discoglossus* (Pugener and Maglia 1997)). According to Ridewood (1897), the ventral cartilage is not observed in the larvae of *Alytes*, *Pelobates*, and *Pipa*.

Interestingly, in an australobatrachian *Calyptocephalella*, the centrum of the 8th presacral vertebra is formed from three ossification centers; paired dorsolateral centers and a mid-ventral element (Muzzopappa et al. 2016). This finding implies that some anurans retain mechanisms inducing ossification at the ventral midline, in addition to the dorsolateral positions.

#### 4.4 | Perichordal and Epichordal Modes in the Evolutionary Context

The general concept of centrum formation in vertebrates is the induction of cartilage by the notochord in the surrounding sclerotomal tissue. Nevertheless, comparative anatomical studies have demonstrated that the skeletal elements constituting the centrum are not singular. In the vertebral column of the shark, the centrum is composed of cartilage layers around the notochord intercalated by additional skeletal elements known as the dorsal arch base and ventral arch base (Romer and Parsons 1977). In the larvae of *Amia*, the centrum has the dorsal arch base at the base of neural arches and the ventral arch base at the base of hemal arches, in addition to cartilage around the notochord. These arch bases are incorporated into the centrum in adult *Amia* (Romer and Parsons 1977).

The centrum of Paleozoic tetrapods had various compositions. This diversity in vertebral composition has long been known in paleontology and comparative anatomy (Romer and Parsons 1977), and recent research expanded to paleohistology (Danto et al. 2016) and morphometric analysis (Carter et al. 2021). Among these animals, including temnospondyls, a pair of pleurocentra at the base of neural arches and a single intercentrum at the ventral midline were the primary components of the centrum. In the lineage leading to reptiles, the pleurocentrum enlarged and occupied most of the centrum, and the intercentrum diminished into a ventrally intercalated small element. Romer and Parsons (1977) described that extant amphibians exhibit neither the pleurocentrum nor the intercentrum and form a simple cylindrical centrum. More recent paleontological findings have established that all extant amphibians are descendants of temnospondyls (Kligman et al. 2023). Among temnospondyls, amphibamids are most closely related to the ancestors of extant amphibians. The centrum of the Permian amphibamid *Doleserpeton* is composed of a large pleurocentrum and a small wedge-like intercentrum (Sigurdson and Bolt 2010). In *Gerobatrachus*, which is closely related to the common ancestors of anurans and urodeles, the intercentrum is reduced to a small piece of bone (Anderson et al. 2008).

In *Triadobatrachus*, a sister group of anurans, the intercentrum is lost, and the centrum is composed of a single cylindrical element (Rage and Rocek 1989). In the *Triadobatrachus* fossil, the bony intercentrum is lost; however, there are certain spaces between consecutive centra, implying the presence of cartilaginous intervertebral tissue similar to that in extant amphibians. In our observations in *R. kobai*, the crescent-shaped cartilage domain was adjacent to the posteroventral corner of the centrum (Figure 4). Traditionally, the intercentrum in temnospondyls has been depicted as being located at the anteroventral corner of the pleurocentrum. However, reinvestigation of the vertebrae of *Ichthyostega* revealed that the intercentrum was located at the posteroventral corner of the pleurocentrum (Pierce et al. 2013). Therefore, the location of the crescent-shaped domain in *R. kobai* is consistent with that of the intercentrum in *Ichthyostega* and several temnospondyls.

Ancestral temnospondyls had mechanisms forming a pair of pleurocentrum at the base of neural arches and mechanisms forming the intercentrum at the ventral midline, in addition to mechanisms forming cartilage around the notochord (Figure 8).

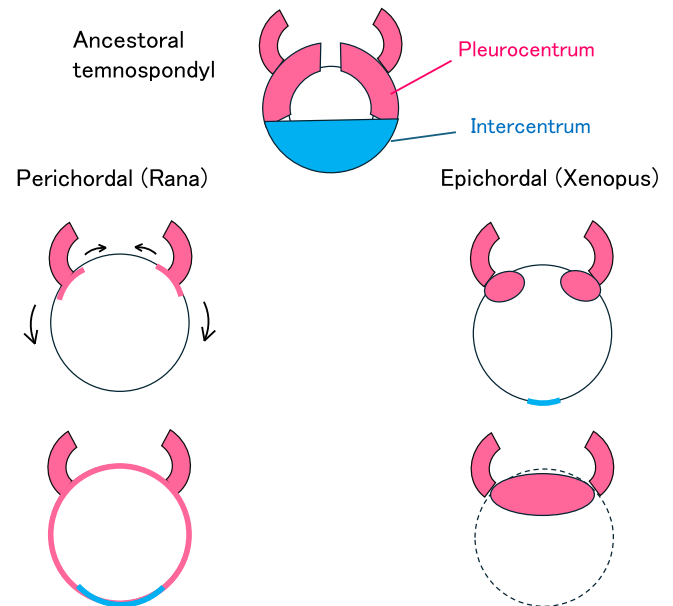


**FIGURE 8** | A hypothesis for the derivation of perichordal and epichordal modes in the evolutionary background. The ancestral temnospondyl had mechanisms forming a pair of pleurocentra at the base of neural arches and an intercentrum at the ventral midline, in addition to the cartilage layer around the notochord. The anuran ancestor lost the pleurocentrum and intercentrum as discrete skeletal elements. However, the mechanisms inducing skeletal elements at the base of neural arches are partially maintained, so that centrum ossification precedes at these regions. In addition, a crescent-shaped cartilage domain is formed at the ventral midline in the intervertebral region. In the epichordal lineage, including *Xenopus*, the trunk notochord tends to regress, and the mechanisms inducing the cartilage layer around the notochord are severely diminished. This promoted the secondary development of pleurocentrum-like skeletal elements at the base of neural arches. Furthermore, the *Xenopus* larva forms a transient cartilage ventral to the notochord. Thus, the difference between perichordal and epichordal modes can be perceived as the difference in the balance between the two mechanisms.



In the anuran ancestors, the pleurocentrum and intercentrum were lost, suggesting that these mechanisms were replaced by mechanisms forming a cylindrical centrum around the notochord. This state probably represents the perichordal mode. However, the mechanisms forming the pleurocentrum at the base of neural arches were partially maintained so that centrum ossification starts from these regions. Otherwise, centrum ossification should proceed uniformly around the notochord. Similarly, the mechanisms forming the intercentrum at the ventral midline also partially persisted, so that the crescent-shaped cartilage domain is formed at the intervertebral region in *Rana*. Conversely, there was a tendency for the loss of the trunk notochord during metamorphosis in epichordal lineages, resulting in the loss of mechanisms inducing cartilage around the notochord in epichordal species such as *Xenopus*. It is possible that this prompted the secondary development of the pleurocentrum-like bony elements at the base of neural arches. Moreover, *Xenopus* larvae exhibited transient ventral cartilage under the notochord (Mookerjee 1931; Nieuwkoop 1956; Takahashi et al. 2024). Thus, the difference between perichordal and epichordal modes may not be related to dorsoventral patterning but related to the balance between the mechanisms inducing bony elements around the notochord and those at the base of neural arches.

As evolutionary history is seldom experimentally reproduced, comparative approaches to known representatives of perichordal and epichordal species are crucial even in the modern day. At the same time, the diversity of centrum formation may provide an attractive theme for evolutionary developmental biology. Recent progress in comparative genome analysis and gene manipulation techniques, such as genome editing, may undoubtedly facilitate understanding of the mechanisms underlying these diversities.

#### Author Contributions

**Yu Takahashi:** conceptualization, methodology, data curation, investigation, writing – original draft, writing – review and editing. **Takeshi Igawa:** resources, writing – review and editing. **Chiyo Nanba:** resources. **Hajime Ogino:** resources. **Hideho Uchiyama:** writing – review and editing. **Satoshi Kitajima:** supervision, funding acquisition, writing – review and editing.

#### Acknowledgments

The authors express gratitude to Prof. Akimasa Fukui at Chuou University for invitation at the academic meeting in Zoological Society in Japan, and to Hiromi Yoshioka at the Cellular and Molecular Toxicology Division for administrative work.

#### Conflicts of Interest

The authors declare no conflicts of interest.

#### Data Availability Statement

The data that support the findings of this study are available from figshare with DOIs below.

[10.6084/m9.figshare.28553123](https://doi.org/10.6084/m9.figshare.28553123)

[10.6084/m9.figshare.28553213](https://doi.org/10.6084/m9.figshare.28553213)

[10.6084/m9.figshare.28553282](https://doi.org/10.6084/m9.figshare.28553282)

[10.6084/m9.figshare.28553339](https://doi.org/10.6084/m9.figshare.28553339)

[10.6084/m9.figshare.28553366](https://doi.org/10.6084/m9.figshare.28553366)

[10.6084/m9.figshare.28553408](https://doi.org/10.6084/m9.figshare.28553408)

[10.6084/m9.figshare.28553465](https://doi.org/10.6084/m9.figshare.28553465)

[10.6084/m9.figshare.28553501](https://doi.org/10.6084/m9.figshare.28553501)

[10.6084/m9.figshare.28562384](https://doi.org/10.6084/m9.figshare.28562384)

In addition, the high-resolution figures in Takahashi et al. (2024) will also be available from figshare.

#### References

- Adolphi, H. 1892. “Über Variationen der Spinalnerven und der Wirbelsäule anurer Amphibien. I. (*Bufo variabilis* Pall.).” *Gegenbaurs Morphologisches Jahrbuch* 19: 313–375.
- Adolphi, H. 1895. “Über Variationen der Spinalnerven und der Wirbelsäule anurer Amphibien. II. (*Pelobates fuscus* Wagl. und *Rana esculenta* L.).” *Gegenbaurs Morphologisches Jahrbuch* 22: 449–490.
- Anderson, J. S., R. R. Reisz, D. Scott, N. B. Fröbisch, and S. S. Sumida. 2008. “A Stem Batrachian From the Early Permian of Texas and the Origin of Frogs and Salamanders.” *Nature* 453, no. 7194: 515–518. <https://doi.org/10.1038/nature06865>.
- Báez, A. M., and L. Nicoli. 2004. “A New Look at an Old Frog: The Jurassic *Notobatrachus Reig* From Patagonia.” *Ameghiniana* 41: 257–270.
- Banbury, B., and A. M. Maglia. 2006. “Skeletal Development of the Mexican Spadefoot, *Spea multiplicata* (Anura: Pelobatidae).” *Journal of Morphology* 267, no. 7: 803–821. <https://doi.org/10.1002/jmor.10441>.
- Blanco, M. J., and B. Sanchiz. 2000. “Evolutionary Mechanisms of Rib Loss in Anurans: A Comparative Developmental Approach.” *Journal of Morphology* 244, no. 1: 57–67. [https://doi.org/10.1002/\(SICI\)1097-4687\(200004\)244:1<57::AID-JMOR6>3.0.CO;2-7](https://doi.org/10.1002/(SICI)1097-4687(200004)244:1<57::AID-JMOR6>3.0.CO;2-7).
- Carter, A. M., S. T. Hsieh, P. Dodson, and L. Sallan. 2021. “Early Amphibians Evolved Distinct Vertebrae for Habitat Invasions.” *PLoS One* 16, no. 6: e0251983. <https://doi.org/10.1371/journal.pone.0251983>.
- Chuliver, M., F. L. Agnolín, A. Scanferla, et al. 2024. “The Oldest Tadpole Reveals Evolutionary Stability of the Anuran Life Cycle.” *Nature* 636: 138–142. <https://doi.org/10.1038/s41586-024-08055-y>.
- Danto, M., F. Witzmann, and N. B. Fröbisch. 2016. “Vertebral Development in Paleozoic and Mesozoic Tetrapods Revealed by Paleohistological Data.” *PLoS One* 11, no. 4: e0152586. <https://doi.org/10.1371/journal.pone.0152586>.
- Frost, D. R. 2024. “Amphibian Species of the World: An Online Reference. Version 6.2,” accessed February 10, 2025, Electronic Database accessible at <http://amphibiansoftheworld.amnh.org/index.php>. American Museum of Natural History, New York, USA. <https://doi.org/10.5531/db.vz.0001>
- Griffiths, I. 1963. “The Phylogeny of the Salientia.” *Biological Reviews* 38, no. 2: 241–292. <https://doi.org/10.1111/j.1469-185x.1963.tb00784.x>.
- Haas, A. 1999. “Larval and Metamorphic Skeletal Development in the Fast-Developing Frog *Pyxicephalus Adspersus* (Anura, Ranidae).” *Zoomorphology* 119: 23–35.
- Haas, A. 2003. “Phylogeny of Frogs as Inferred From Primarily Larval Characters (Amphibia:Anura).” *Cladistics* 19, no. 1: 23–89. <https://doi.org/10.1111/j.1096-0031.2003.tb00405.x>.
- Haas, A., S. Hertwig, and I. Das. 2006. “Extreme Tadpoles: The Morphology of the Fossorial Megophryid Larva, *Leptobranchella mjobergi*.” *Zoology* 109, no. 1: 26–42. <https://doi.org/10.1016/j.zool.2005.09.008>.

- Haas, A., S. Schwippert, S. Busse, et al. 2021. "Anomalies in the Vertebral Column and Ilio-Sacral Articulation of Some Anuran Amphibians." *Salamandra* 57, no. 1: 53–64.
- Hall, J. A., and J. H. Larsen, Jr. 1998. "Postembryonic Ontogeny of the Spadefoot Toad, *Scaphiopus intermontanus* (Anura: Pelobatidae): Skeletal Morphology." *Journal of Morphology* 238, no. 2: 179–244. [https://doi.org/10.1002/\(SICI\)1097-4687\(199811\)238:2<179::AID-JMOR4>3.0.CO;2-6](https://doi.org/10.1002/(SICI)1097-4687(199811)238:2<179::AID-JMOR4>3.0.CO;2-6).
- Handrigan, G. R., A. Haas, and R. J. Wassersug. 2007. "Bony-Tailed Tadpoles: The Development of Supernumerary Caudal Vertebrae in Larval Megophryids (Anura)." *Evolution & Development* 9, no. 2: 190–202. <https://doi.org/10.1111/j.1525-142X.2007.00149.x>.
- Handrigan, G. R., and R. J. Wassersug. 2007a. "The Anuran Bauplan: A Review of the Adaptive, Developmental, and Genetic Underpinnings of Frog and Tadpole Morphology." *Biological Reviews of the Cambridge Philosophical Society* 82, no. 1: 1–25. <https://doi.org/10.1111/j.1469-185X.2006.00001.x>.
- Handrigan, G. R., and R. J. Wassersug. 2007b. "The Metamorphic Fate of Supernumerary Caudal Vertebrae in South Asian Litter Frogs (Anura: Megophryidae)." *Journal of Anatomy* 211, no. 3: 271–279. <https://doi.org/10.1111/j.1469-7580.2007.00757.x>.
- Kemp, N. E., and J. A. Hoyt. 1969. "Sequence of Ossification in the Skeleton of Growing and Metamorphosing Tadpoles of *Rana pipiens*." *Journal of Morphology* 129, no. 4: 415–443. <https://doi.org/10.1002/jmor.1051290404>.
- Kligman, B. T., B. M. Gee, A. D. Marsh, et al. 2023. "Triassic Stem Caecilian Supports Dissorophoid Origin of Living Amphibians." *Nature* 614, no. 7946: 102–107. <https://doi.org/10.1038/s41586-022-05646-5>.
- Maglia, A. M., and L. A. Pugener. 1998. "Skeletal Development and Adult Osteology of *Bombina Orientalis* (Anura: Bombinatoridae)." *Herpetologica* 54: 344–363.
- Meza-joya, F. L., E. P. Ramos-pallares, and M. P. Ramírez-pinilla. 2013. "Ontogeny of the Vertebral Column of *Eleutherodactylus johnstonei* (Anura: Eleutherodactylidae) Reveals Heterochronies Relative to Metamorphic Frogs." *Anatomical Record* 296, no. 7: 1019–1030. <https://doi.org/10.1002/ar.22705>.
- Mookerjee, H. K. 1931. "On the Development of the Vertebral Column of Anura." *Philosophical Transactions of the Royal Society of London, Series B: Biological Sciences* 219: 165–195.
- Muzzopappa, P., L. A. Pugener, and A. M. Báez. 2016. "Postcranial Osteogenesis of the Helmeted Water Toad *Calyptocephalella gayi* (Neobatrachia: Calyptocephalellidae) With Comments on the Osteology of Australobatrachians." *Journal of Morphology* 277, no. 2: 204–230. <https://doi.org/10.1002/jmor.20490>.
- Nicholls, G. E. 1916. "The Structure of the Vertebral Column in the Anura *Phaneroglossa* and its Importance as a Basis of Classification." *Proceedings of the Linnean Society of London* 128: 80–92.
- Nieuwkoop, P. D., and J. Faber. 1956. *Normal Table of Xenopus laevis (Daudin). A Systematical and Chronological Survey of the Development From the Fertilized Egg Till the End of Metamorphosis*. North-Holland Publishing.
- Noble, G. K. 1922. "The Phylogeny of the Salientia. I. The Osteology and the Thigh Musculature; Their Bearing on Classification and Phylogeny." *Bulletin of the American Museum of Natural History* 46: 1–87.
- Pierce, S. E., P. E. Ahlberg, J. R. Hutchinson, et al. 2013. "Vertebral Architecture in the Earliest Stem Tetrapods." *Nature* 494, no. 7436: 226–229. <https://doi.org/10.1038/nature11825>.
- Púgener, L. A., and A. M. Maglia. 1997. "Osteology and Skeletal Development of *Discoglossus sardus* (Anura: Discoglossidae)." *Journal of Morphology* 233, no. 3: 267–286. [https://doi.org/10.1002/\(SICI\)1097-4687\(199709\)233:3<267::AID-JMOR6>3.0.CO;2-0](https://doi.org/10.1002/(SICI)1097-4687(199709)233:3<267::AID-JMOR6>3.0.CO;2-0).
- Pugener, L. A., and A. M. Maglia. 2009. "Skeletal Morphogenesis of the Vertebral Column of the Miniature Hyliid Frog *Acris crepitans*, With Comments on Anomalies." *Journal of Morphology* 270, no. 1: 52–69. <https://doi.org/10.1002/jmor.10665>.
- Rage, J.-C., and Z. Roček. 1989. "Redescription of *Triadobatrachus massinoti* (Piveteau, 1936) an Anuran Amphibian From the Early Triassic." *Palaeontographica Abteilung A* 206: 1–16.
- Ridewood, W. G. 1897. "On the Development of the Vertebral Column in *Pipa* and *Xenopus*." *Anatomischer Anzeiger* 13: 359–376.
- Romer, A. S., and T. S. Parsons. 1977. *The Vertebrate Body*. 5th ed. Saunders.
- Ročková, H., and Z. Roček. 2005. "Development of the Pelvis and Posterior Part of the Vertebral Column in the Anura." *Journal of Anatomy* 206, no. 1: 17–35. <https://doi.org/10.1111/j.0021-8782.2005.00366.x>.
- Senevirathne, G., S. Garg, R. Kerney, M. Meegaskumbura, and S. D. Biju. 2016. "Unearthing the Fossorial Tadpoles of the Indian Dancing Frog Family Micrixalidae." *PLoS One* 11, no. 3: e0151781. <https://doi.org/10.1371/journal.pone.0151781>.
- Sheil, C. A., and H. Alamillo. 2005. "Osteology and Skeletal Development of *Phyllomedusa Vaillantii* (Anura: Hylidae: Phyllomedusinae) and a Comparison of This Arboreal Species With a Terrestrial Member of the Genus." *Journal of Morphology* 265, no. 3: 343–368. <https://doi.org/10.1002/jmor.10362>.
- Sigurdson, T., and J. R. Bolt. 2010. "The Lower Permian Amphibamid *Doloserpeton* (Temnospondyli: Dissorophoidea), the Interrelationships of Amphibamids, and the Origin of Modern Amphibians." *Journal of Vertebrate Paleontology* 30, no. 5: 1360–1377.
- Soliz, M., and M. L. Ponssa. 2016. "Development and Morphological Variation of the Axial and Appendicular Skeleton in Hylidae (Lissamphibia, Anura)." *Journal of Morphology* 277, no. 6: 786–813. <https://doi.org/10.1002/jmor.20536>.
- Tahara, Y. 1974. "Table of the Normal Developmental Stages of the Frog, *Rana japonica*. II. Late Development (Stages 26–40)." *Memoirs of Osaka Kyoiku University III, Natural Science and Applied Science* 23: 33–53.
- Takahashi, Y., R. Wakabayashi, S. Kitajima, and H. Uchiyama. 2024. "Epichordal Vertebral Column Formation in *Xenopus laevis*." *Journal of Morphology* 285, no. 2: e21664. <https://doi.org/10.1002/jmor.21664>.
- Trueb, L., and J. Hanken. 1992. "Skeletal Development in *Xenopus laevis* (Anura: Pipidae)." *Journal of Morphology* 214, no. 1: 1–41. <https://doi.org/10.1002/jmor.1052140102>.
- Trueb, L., L. Pugener, and A. M. Maglia. 2000. "Ontogeny of the Bizarre: An Osteological Description of *Pipa pipa* (Anura: Pipidae), With an Account of Skeletal Development in the Species." *Journal of Morphology* 243, no. 1: 75–104. [https://doi.org/10.1002/\(SICI\)1097-4687\(200001\)243:1<75::AID-JMOR4>3.0.CO;2-L](https://doi.org/10.1002/(SICI)1097-4687(200001)243:1<75::AID-JMOR4>3.0.CO;2-L).
- Vera, M. C., and M. L. Ponssa. 2014. "Skeletogenesis in Anurans: Cranial and Postcranial Development in Metamorphic and Post-metamorphic Stages of *Leptodactylus bufonius* (Anura: Leptodactylidae)." *Acta Zoologica* 95: 44–62.
- Wiens, J. J. 1989. "Ontogeny of the Skeleton of *Spea bombifrons* (Anura: Pelobatidae)." *Journal of Morphology* 202, no. 1: 29–51. <https://doi.org/10.1002/jmor.1052020104>.
- Yasutake, J., K. Inohaya, and A. Kudo. 2004. "Twist Functions in Vertebral Column Formation in Medaka, *Oryzias latipes*." *Mechanisms of Development* 121, no. 7–8: 883–894. <https://doi.org/10.1016/j.mod.2004.03.008>.
- Коваленко, Е. Е., and Ю. И. Кружкова. 2013. "Индивидуальная Изменчивость Развития Серой Жабы *Bufo bufo* (Anura, Bufonidae). 2. Диагностические Признаки Осевого Скелета." *Онтогенез* 44, no. 4: 249–264. <https://doi.org/10.7868/s0475145013040058>.